Electronic Supplementary Material to: Impacts of Anthropogenic Forcings and El Niño on Chinese Extreme Temperatures*

N. FREYCHET[1], S. SPARROW[2], S. F. B. TETT[1], M. J. MINETER[1], G. C. HEGERL[1], and D. C. H. WALLOM[2]

[1]*School of Geosciences, University of Edinburgh, Crew Building, The King's Buildings, Edinburgh* EH9 3FF, *UK*
[2]*Oxford e-Research Centre, University of Oxford, Oxford,* OX1 2JD, United Kingdom

ESM to: Freychet, N., S. Sparrow, S. F. B. Tett, M. J. Mineter, G. C. Hegerl, and D. C. H. Wallom, 2018: Impacts of anthropogenic forcings and El Niño on Chinese extreme temperatures. *Adv. Atmos. Sci.*, **35**(8), 994–1002, https://doi.org/10.1007/s00376-018-7258-8.

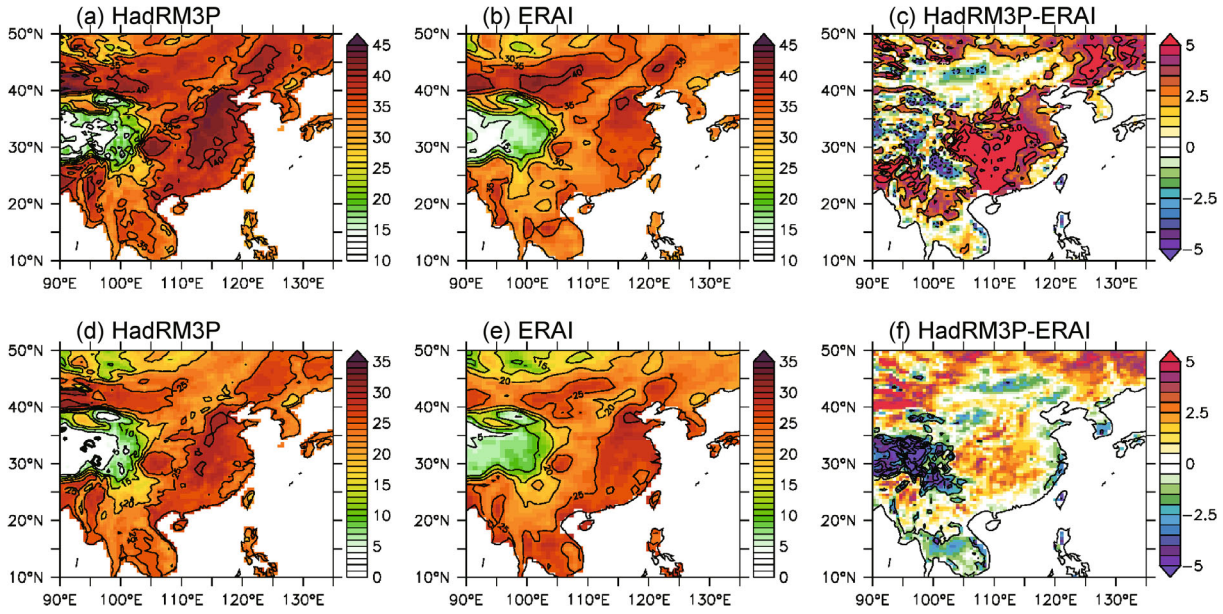

Fig. S1. 2014 daily (a–c) TXx and (d–f) TNx of HadRM3P (ensemble mean of the climatological runs) and the corresponding year of ERA-Interim. For the differences between HadRM3P and ERA-Interim, in (c) and (f), the temperatures of ERA-Interim are first interpolated over the model grid. All units are in °C.

*The online version of this article can be found at https://doi.org/10.1007/s00376-018-7258-8.

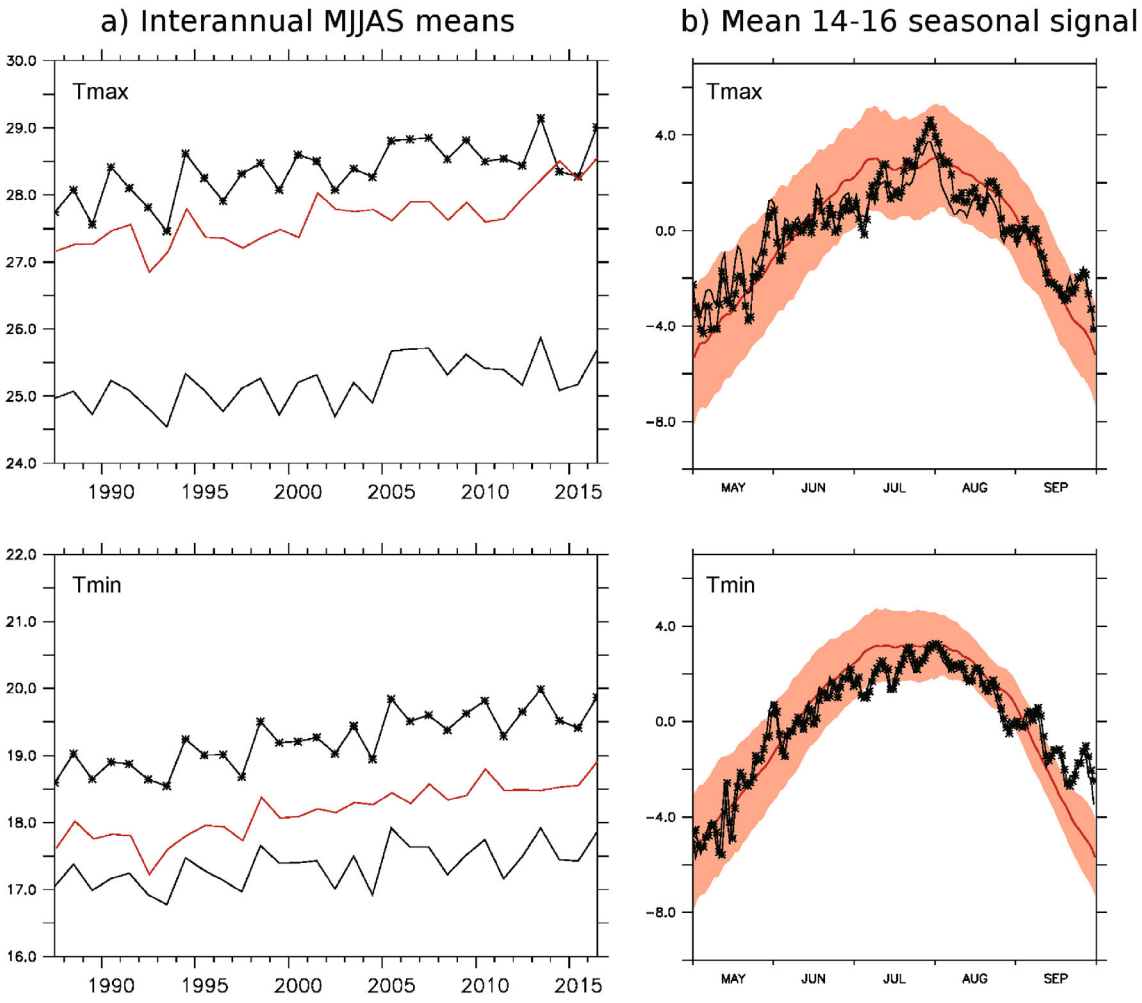

Fig. S2. (a) Central East China (20°–40°N, 100°–125°E) summer (May–September, MJJAS) means for Tmax and Tmin. (b) Mean 2014–16 seasonal signal of Tmax and Tmin (averaged over central East China) relative to the mean MJJAS. Each panel shows: ERA-Interim (black line); homogenized ground station observation (black line with cross symbols); and the ensemble mean of HadRM3P (red line). In (b), the orange shading indicates the ensemble standard deviation. All units are in °C.

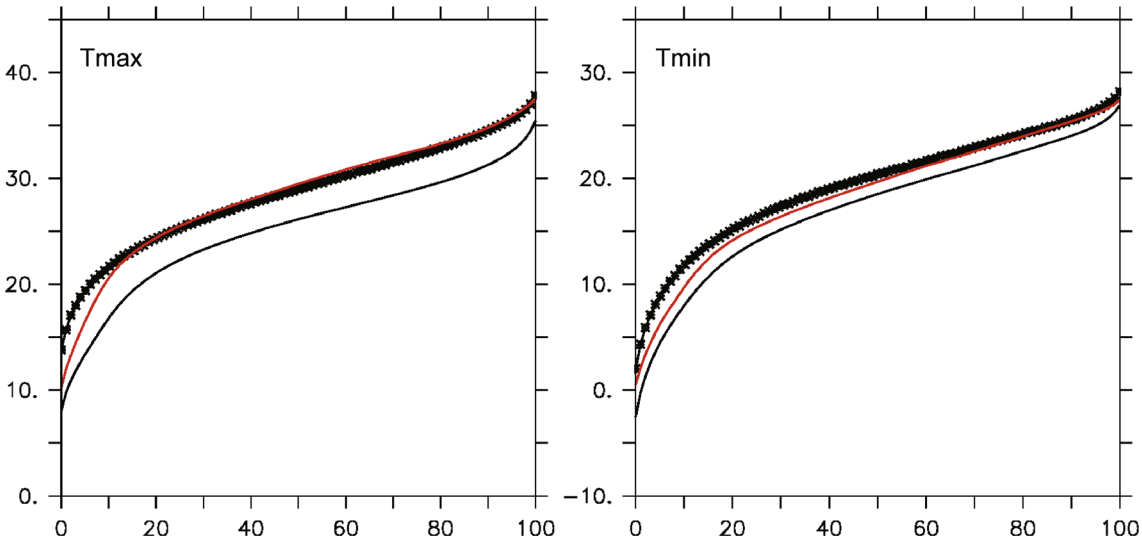

Fig. S3. Percentile distribution of Tmax and Tmin for ERA-Interim (black line), ground station observations (red line), and HadRM3P (black line with cross symbols). The distribution is based on local and daily temperatures over central East China for the extended summers (May–September) of 2014–16.

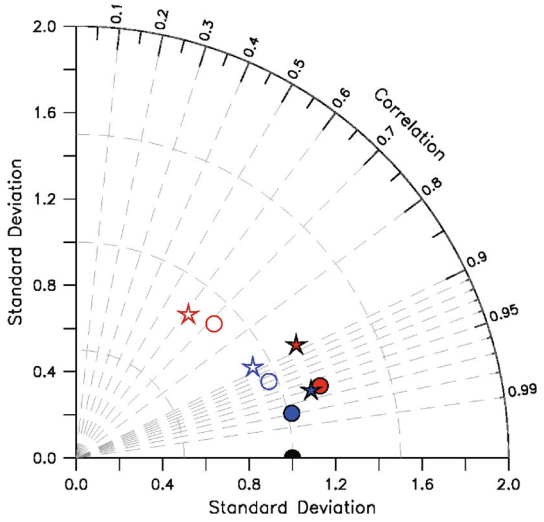

Fig. S4. Taylor diagram representation of the spatial correlation and standard deviation of Tmax (red circle), Tmin (blue circle), TXx (red stars) and TNx (blue stars), based on the 2014–16 summer mean. Empty and filled symbols correspond to ground station observations and HadRM3P, respectively. The reference is ERA-Interim, shown by the black circle.

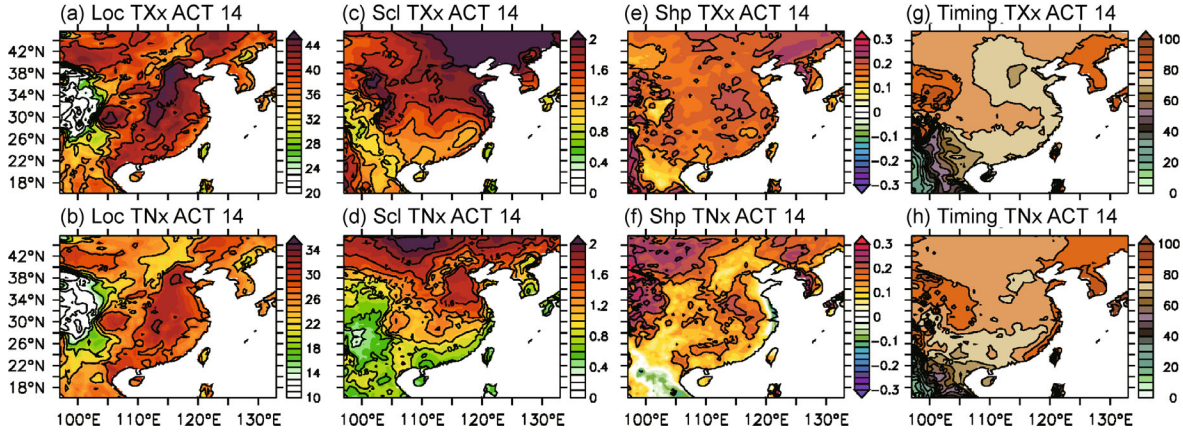

Fig. S5. The (a, b) location (loc; units: °C), (c, d) scale (scl; units: °C) and (e, f) shape (shp; dimensionless) from the GEV fit for TXx and TNx in the ACT-14 ensemble, and the average timing of (g) TXx and (h) TNx relative to 1 May.

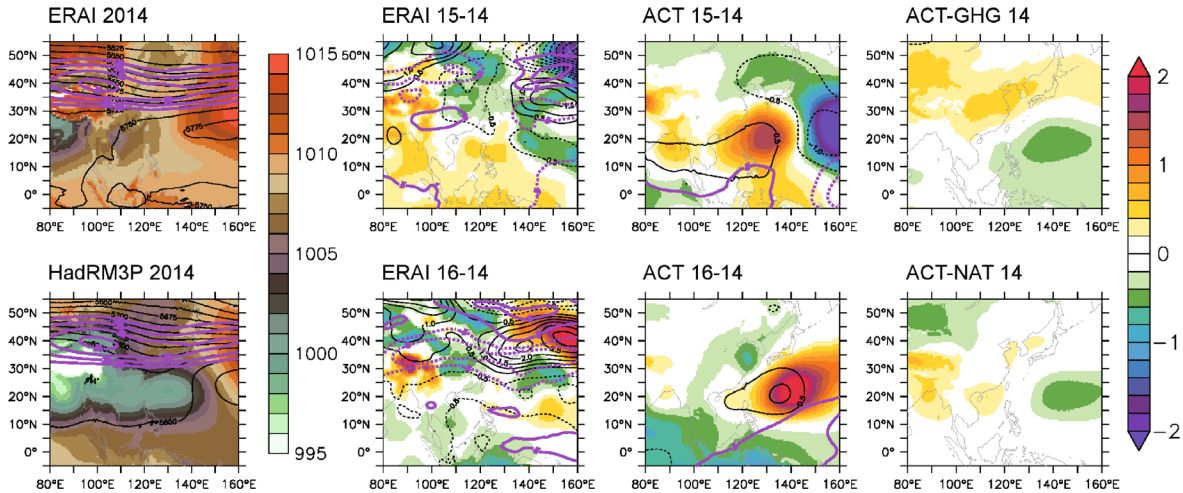

Fig. S6. Left-hand panels: 2014 summer mean sea level pressure (shading; units: Pa), zonal wind at 200 hPa (purple contours; units: m s^{-1}) and 500 hPa geopotential height (black contours; units: m) for ERA-Interim (upper) and HadRM3P (lower). Right-hand panels: Difference between years 2014, 2015 and 2016 for ERA-Interim (left-hand column) and the ACT ensemble mean (middle column), and the difference between the HadRM3P ensemble means (ACT, GHG and NAT) for the year 2014. Variables are similar to the left-hand panels but expressed as differences. To compute the differences of the geopotential height, the regional mean is first removed to prevent any difference due to thermal expansion.

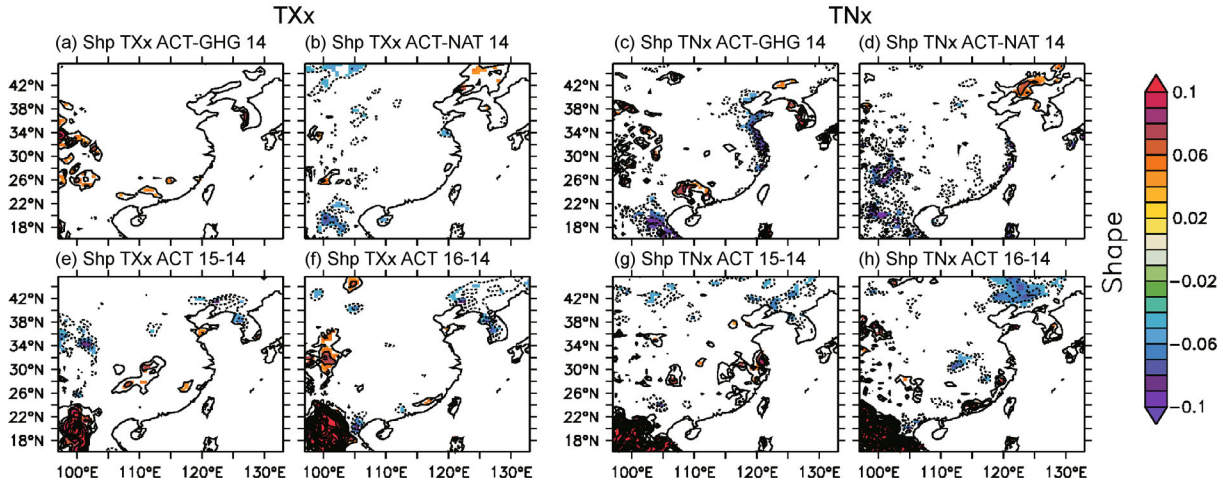

Fig. S7. Differences in the shape parameter from the GEV fit for each ensemble (units: dimensionless). Only significant differences are shaded (see section 2 for details).

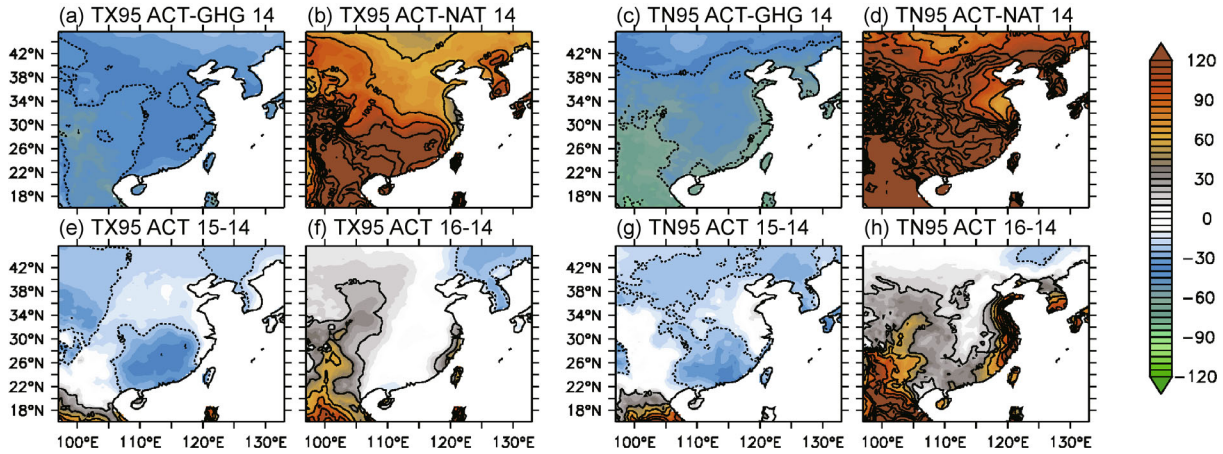

Fig. S8. Difference in the ensemble means of TX95 and TN95. Units: percentage relative to the reference. Contours are every 20% (with dashed lines indicating negative values).

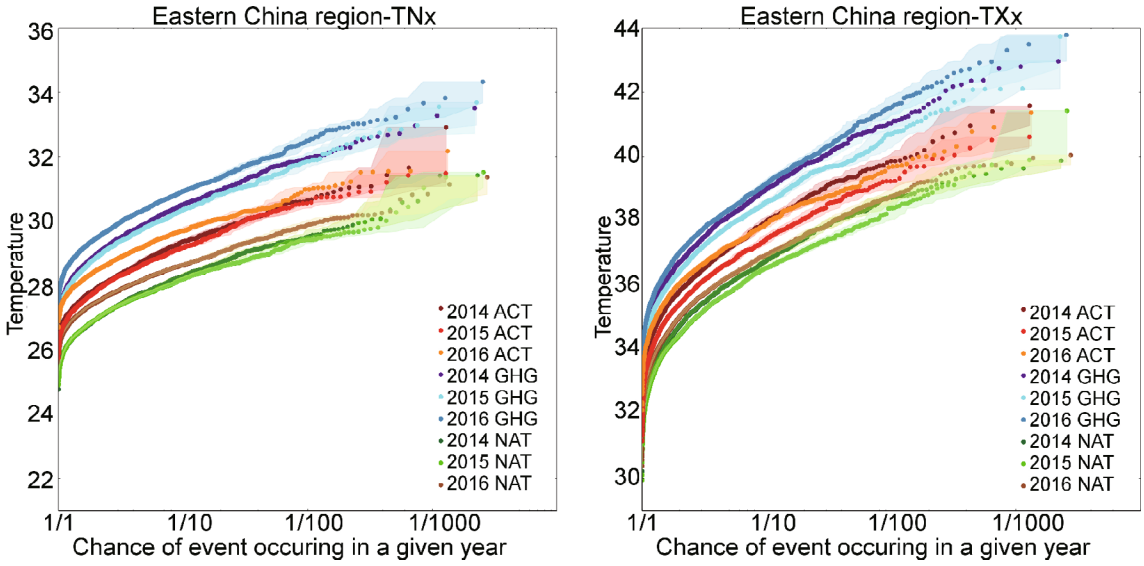

Fig. S9. As in Fig. 3 but for the coastal East China region (25°–35°N, 117°–122°E).